Supporting Information

Bifunctional Ni-TiO_2 Catalyst for Efficient Glycolysis of Polylactic Acid: A Selective Route to Obtain 2-Hydroxyethyl Lactate

Kamlesh Kumari, Shadab Khan and Venkata Krishnan*
School of Chemical Sciences and Advanced Materials Research Center,
Indian Institute of Technology Mandi, Kamand, Mandi 175075, Himachal Pradesh, India.
Email: vkn@iitmandi.ac.in

Sl. No.	Contents	Pg. No.
1	**S1.** Materials characterization	S-2
2	**Figure S1.** PXRD plot of different wt% Ni-TiO_2 catalyst.	S-3
3	**Figure S2.** TGA plot of Ni NP, TiO_2 and Ni-TiO_2 catalyst.	S-4
4	**Figure S3.** PXRD plot of recovered Ni NP after TGA analysis.	S-5
5	**Figure S4.** (a, b) PXRD plot of calcined 20 wt% Ni-TiO_2 catalyst at different temperature (100 °C – 500 °C).	S-6
6	**Figure S5.** Survey spectrum showing presence of all the constituent elements in Ni NP, TiO_2 and Ni-TiO_2.	S-7
7	**Table S1.** Atomic percentage of constituent elements in Ni, TiO_2 and Ni-TiO_2 catalysts from XPS analysis.	S-8
8	**Figure S6.** (a,d,g) N_2 adsorption-desorption isotherms, (b,e,h) BJH pore size distribution and (c,f,i) BET surface area plots for Ni NP, TiO_2 and Ni-TiO_2.	S-9
9	**Table S2.** Amount of acidic and basic sites present in Ni NP, TiO_2 and Ni-TiO_2 catalysts from TPD analysis.	S-10
10	**Table S3.** Control Studies	S-11
11	**Figure S7.** Control reactions for the determination of the role of acidic and basic sites (glycolysis of PLA with (a) benzoic acid and (b) pyridine).	S-12
12	**Figure S8.** FTIR spectrum of benzoic acid and pyridine treated Ni-TiO_2 catalyst.	S-13
13	**Table S4.** Atomic percentage of constituent elements in fresh and recovered Ni-TiO_2 catalysts from XPS analysis.	S-14
14	**S2.** Conversion and Yield Calculations	S-15
15	**S3.** Green Metrics Calculations	S-16
16	**Table S5.** Material input-output and mass-balance analysis for glycolysis of PLA	S-17
17	**S4.** NMR Spectra	S-18

S1. Materials characterization

Various instruments were used to perform different characterizations of the developed catalysts. The powder X-ray diffraction (PXRD) measurements of the catalysts were performed using 9 kW Rigaku Smart Lab rotating anode X-ray diffractometer equipped with Ni-filtered Cu K_α irradiation source having $\lambda = 1.542$ Å working at 45 kV and 100 mA. All the measurements were done at a scattering range of $2\theta = 10°$ to $90°$ with a scanning rate of 2° per min and scan step size of 0.02°. The crystalline phases of the catalysts were identified by JCPDS data obtained from X'Pert HighScore software. An Agilent K8002AA Cary 660 instrument was used to perform Fourier-transform infrared spectroscopy (FTIR) measurements. The thermogravimetric analysis (TGA) of the samples was done using PerkinElmer Pyris 1 instrument. All samples were heated in a nitrogen atmosphere with a flow rate of 20 mL min^{-1} from 25 ^{o}C to 800 ^{o}C with the ramp rate of 10 ^{o}C min^{-1}. The FEI Nova SEM-450 scanning electron microscope (SEM) was utilized for the morphological investigation of the catalyst. The samples were prepared by dispersing 2 mg of catalyst in ethanol, sonicating them for 30 min and drop casting them onto a small piece of silicon wafer. The nanoscale morphological analysis of the samples was performed using a transmission electron microscope (TEM), FEI Tecnai G2 20 S-twin microscope operating at 200 kV accelerating voltage and the d-spacing were calculated using Gatan software. The samples were prepared by dispersing the catalyst in ethanol by ultrasonication for 30 min and drop casting them onto a copper grid having carbon coating. X-ray photoelectron spectroscopy (XPS) studies on the samples were conducted using a Thermo Fisher Scientific NEXSA photoemission spectrometer equipped with 1486.6 eV Al-K_α X-ray radiation source. Brunauer–Emmett–Teller (BET) specific surface area was measured on a Quantachrome ASiQwin instrument at 77.35 K temperature. The samples were degassed under vacuum by heating at 120 ^{o}C with heating rate of 5 ^{o}C min^{-1} before measuring the surface area. Using BELCAT II TPR/TPD, Quanta Chrome instrument the temperature programmed desorption (TPD) study was carried out. Nuclear magnetic resonance (NMR) experiments were performed using a JEOL-USA (JNMECX500) spectrometer in DMSO-D_6 solvent having tetramethyl silane (TMS) as an internal standard and the chemical shifts are reported in ppm. The ^{1}H NMR spectra was recorded at 500 MHz and ^{13}C NMR spectra was recorded at 125 MHz frequency and the data obtained was analyzed using MestReNova software.

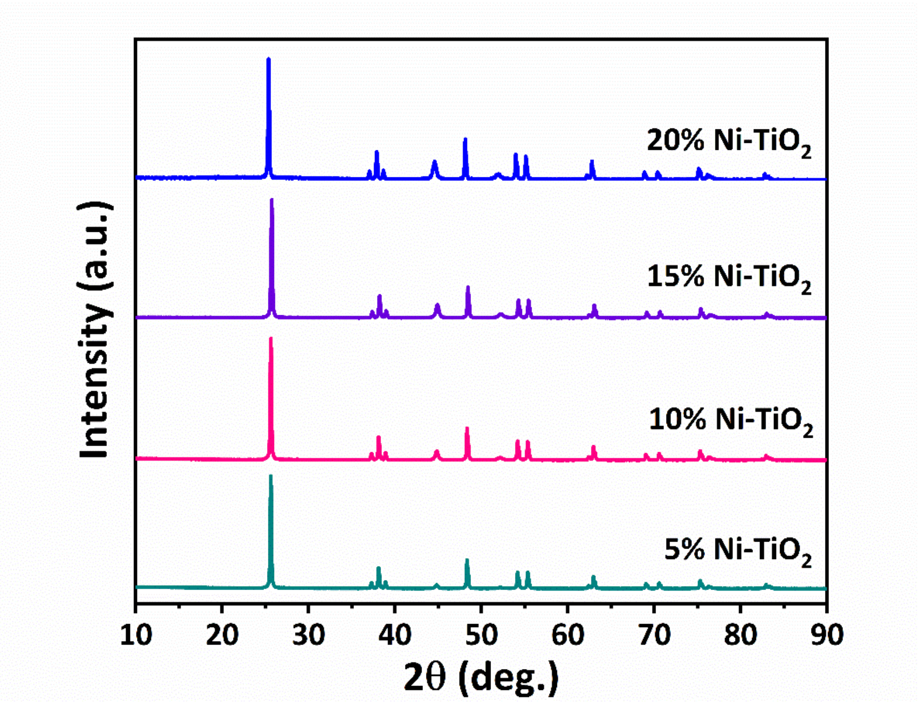

Figure S1. PXRD plot of different wt% Ni-TiO_2 catalyst.

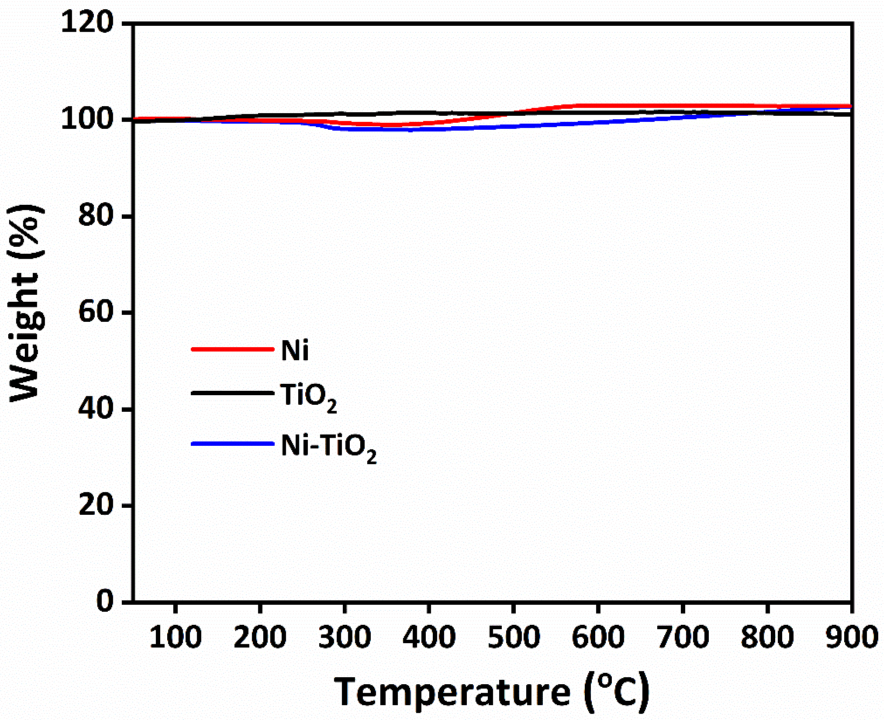

Figure S2. TGA plot of Ni NP, TiO_2 and Ni-TiO_2 catalyst.

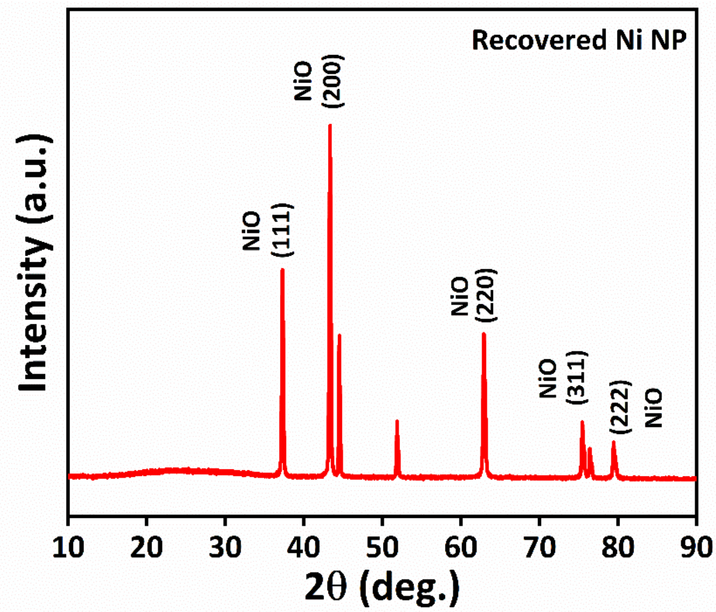

Figure S3. PXRD plot of recovered Ni NP after TGA analysis.

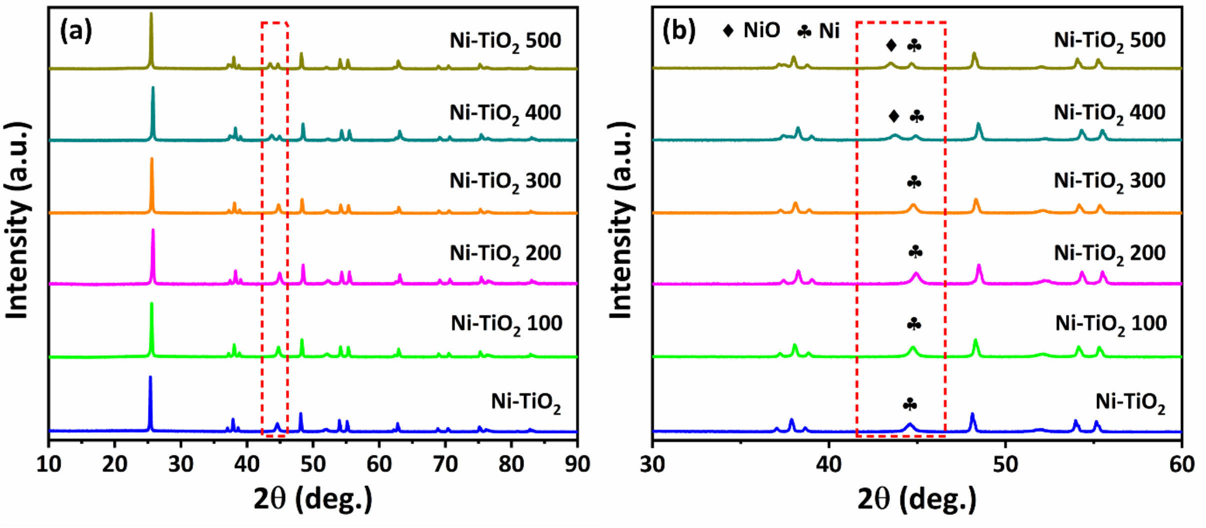

Figure S4. (a, b) PXRD plot of calcined 20 wt% Ni-TiO_2 catalyst at different temperature (100 °C – 500 °C).

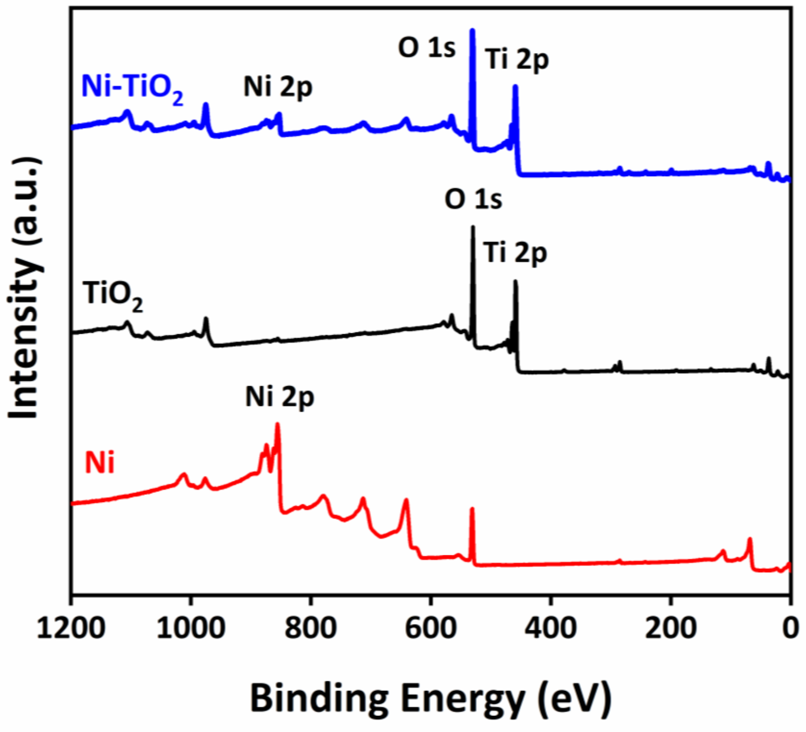

Figure S5. Survey spectrum showing presence of all the constituent elements in Ni NP, TiO_2 and Ni-TiO_2.

Table S1. Atomic percentage of constituent elements in Ni, TiO_2 and Ni-TiO_2 catalysts from XPS analysis.

Sl. No.	**Elements**	**Atomic percentage of constituent elements (%)**		
		Ni	**TiO_2**	**Ni-TiO_2**
1	Ni 2p	86.91	-	7.14
2	Ti 2p	-	33.28	25.46
3	O 1s	13.09	25.46	67.39

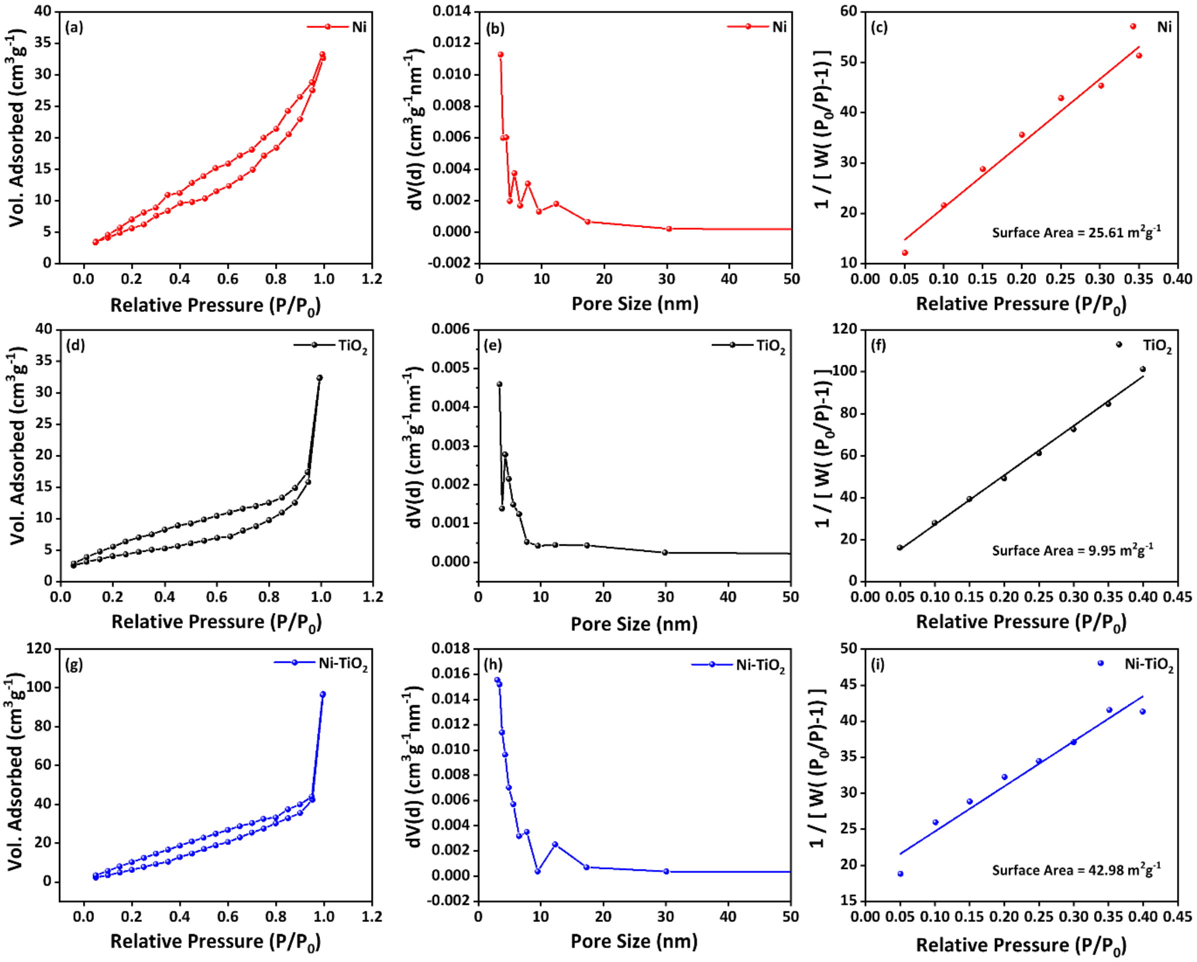

Figure S6. (a,d,g) N_2 adsorption-desorption isotherms, (b,e,h) BJH pore size distribution and (c,f,i) BET surface area plots for Ni NP, TiO_2 and Ni-TiO_2.

Table S2. Amount of acidic and basic sites present in Ni NP, TiO_2 and Ni-TiO_2 catalysts from TPD analysis.

Sl. No.	**Catalysts**	**No. of acidic sites (mmol g^{-1})**	**No. of basic sites (mmol g^{-1})**
1	Ni NP	0.976	1.224
2	TiO_2	0.115	0.178
3	Ni-TiO_2	0.402	0.387

Table S3. Control Studies

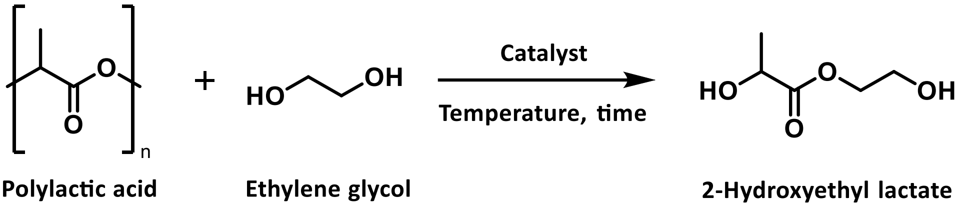

Entry	Catalyst	Temperature (°C)	Time (h)	2-HEtLa yield (%)
1	Ni NP	190	8	63
2	TiO_2	190	8	37
3	Without catalyst	190	8	14

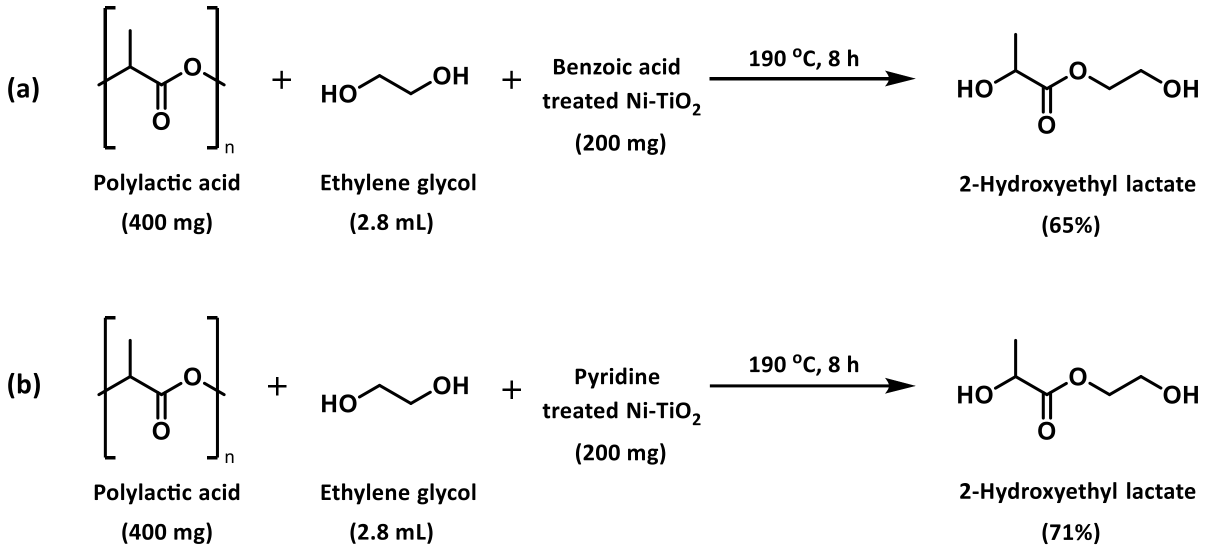

Figure S7. Control reactions for the determination of the role of acidic and basic sites (glycolysis of PLA with (a) benzoic acid treated Ni-TiO_2 and (b) pyridine treated Ni-TiO_2).

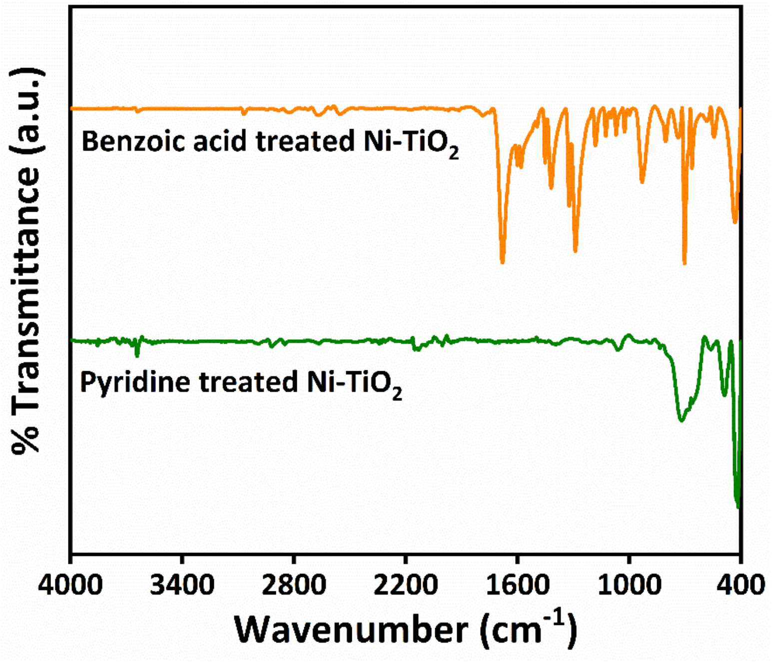

Figure S8. FTIR spectrum of benzoic acid and pyridine treated Ni-TiO$_2$ catalyst.

Table S4. Atomic percentage of constituent elements in fresh and recovered Ni-TiO_2 catalysts from XPS analysis.

Sl. No.	**Elements**	**Atomic percentage of constituent elements (%)**	
		Fresh Ni-TiO_2	**Recovered Ni-TiO_2**
1	Ni 2p	7.14	7.16
2	Ti 2p	25.46	25.40
3	O 1s	67.39	67.43

S2. Yield Calculations

To quantify the yield of 2-HEtLa formed, NMR method is used wherein 1,1,2,2-tetrachloroethane is used as an internal standard. For the NMR analysis, 105 µL of internal standard, 600 µL DMSO-D_6 was added to the concentrated reaction mixture. The yield was calculated by the integration of NMR peaks of the 2-HEtLa with respect to the internal standard using this formula.

$$\frac{Number\ of\ moles\ of\ product}{Number\ of\ moles\ of\ internal\ standard} = \frac{\frac{Integral\ area\ of\ product\ peak}{Number\ of\ protons\ corresponding\ \ to\ peak}}{\frac{Integral\ area\ of\ internal\ standard\ peak}{Number\ of\ proton\ corresponding\ to\ peak}}$$

$$Yield\ (\%) = \frac{Number\ of\ moles\ of\ product}{Number\ of\ moles\ of\ reactant} \times 100$$

S3. Green Metric Calculations

(1) Energy Economy Coefficient (ε): ε is a measure of energy efficiency of the reaction by comparing energy consumption to the reaction output. The ε coefficient relates the yield of the main monomer produced from each depolymerization process with the time and temperature required for the reaction. The lower the temperature and the reaction time, the higher the relative value of the ε coefficient.

$$\mathcal{E} = \frac{Y}{T\times t}$$

$$= \frac{0.98}{190\times 480} = 1.07\times 10^{-5}\ {}^{o}\mathrm{C}^{-1}\ \mathrm{min}^{-1}$$

where T is the reaction temperature in degrees Celsius, t is the reaction time (in minutes) and Y is the yield of the main monomer in mass fraction.

(2) Environmental Factor (E_{factor}): E-factor defines the ratio of mass of waste to mass of product. It implies how much waste is generated in a chemical process. For an ideal green chemical reaction, E-factor should be 0. Higher the E-factor means a greater amount of waste is generated which can have a detrimental impact on the environment.

$$E_{factor} = \frac{mass\ of\ waste}{mass\ of\ product}$$

$$= \frac{[0.35\times\left(\frac{Solvent}{PLA}ratio\right)+\left(\frac{Catalyst}{PLA}ratio\right)+\left(other\frac{Subst}{PLA}ratio\right)]\times m_{PLA}}{Yield_{Product}\times\frac{MM_{product}}{MM_{PLA}}\times m_{PLA}}$$

$$= \frac{[0.35\times\left(\frac{3.11}{0.4}\right)+\left(\frac{0.2}{0.4}\right)+(0)]\times 72.06}{0.98\times\frac{134.13}{72.06}\times 72.06}$$

$$= 1.765$$

In this calculation, the solvent contribution is multiplied by 0.35 as 65% of solvent (ethylene glycol) was recycled, while DCM extraction and associated solvent losses were not included.

(3) Environment Energy Impact Factor (ξ): ξ would measure the environmental impact associated with the energy used in the depolymerization process. It takes into consideration both the energy economy coefficient and environmental factor. A lower ξ would indicate a more environmentally friendly and energy-efficient depolymerization process.

$$\xi = \frac{E_{factor}}{\varepsilon} = \frac{1.765}{1.07\times 10^{-5}} = 1.65\times 10^{5}\ {}^{o}\mathrm{C}\ \mathrm{min}$$

Table S5. Material input-output and mass-balance analysis for glycolysis of PLA

Sl. No.	**Input (g)**	**Output (g)**
1.	PLA = 0.400 g	2-HEtLa = 0.643 g
2.	Ethylene glycol = 3.110 g	Recovered ethylene glycol = 2.029 g
3.	Catalyst amount = 0.200 g	Catalyst recovered = 0.190 g
4.	Total = 3.710 g	Total = 2.862 g

$$\text{Mass Balance (\%)} = \frac{Total\ Output}{Total\ Input} \times 100$$

$$\text{Mass Balance (\%)} = \frac{2.862}{3.710} \times 100$$

Mass Balance (%) = 76.36%

S4. NMR Spectra

^{1}H-NMR spectrum of 2-HEtLa [500 MHz, DMSO-D$_6$]

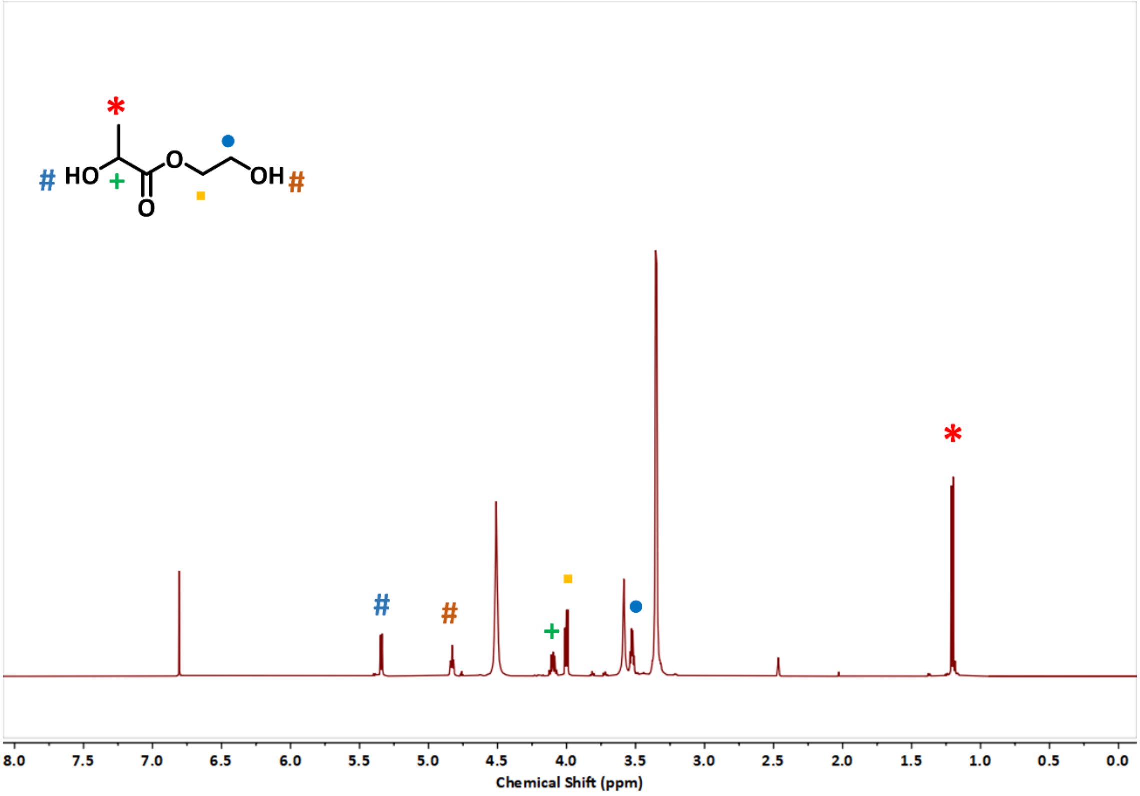

^{13}C-NMR spectrum of 2-HEtLa [125 MHz, DMSO-D$_6$]